Universiteit
Leiden
The Netherlands

Gene therapy strategies to target post-interventional vascular remodeling

Eefting, D.

Citation
Eefting, D. (2009, November 4). *Gene therapy strategies to target post-interventional vascular remodeling*. Retrieved from https://hdl.handle.net/1887/14324

Version:	Corrected Publisher's Version
License:	Licence agreement concerning inclusion of doctoral thesis in the Institutional Repository of the University of Leiden
Downloaded from:	https://hdl.handle.net/1887/14324

Note: To cite this publication please use the final published version (if applicable).

Color supplement

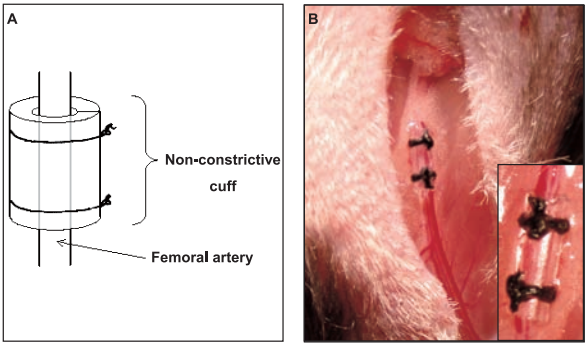

Figure 1.2. Schematic representation (A) and microphotograph (B) of femoral artery cuff positioning.

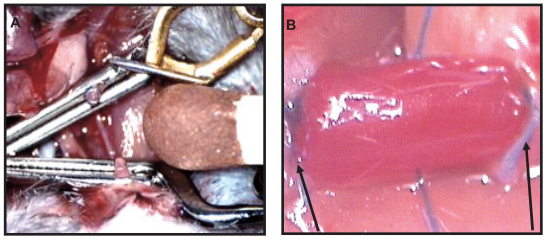

Figure 1.3. Panel A: Vein graft model in a mouse. The common carotid artery is divided and temporarily clamped to obtain haemostasis. The (donor) caval vein will be placed as an interponate into the carotid artery. Panel B: Venous interponate in situ, arrows indicate anastomotic side.

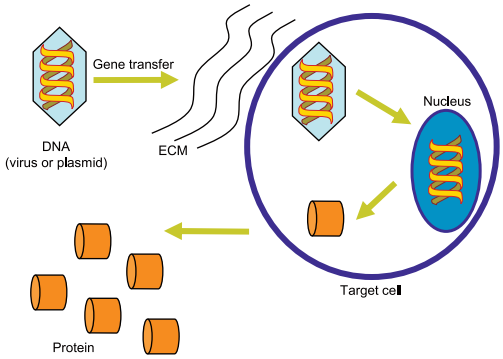

Figure 1.4. Schematic mechanism for gene therapy

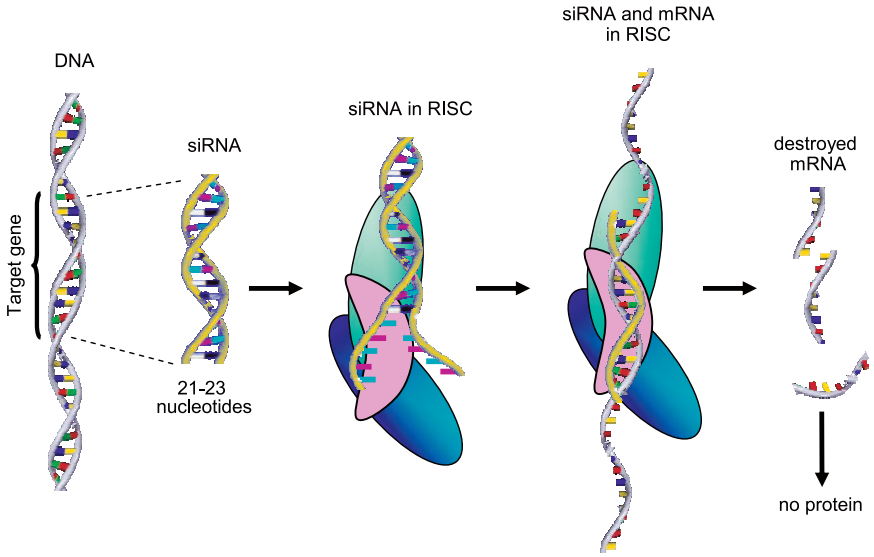

Figure 1.5. Mechanism for RNA interference

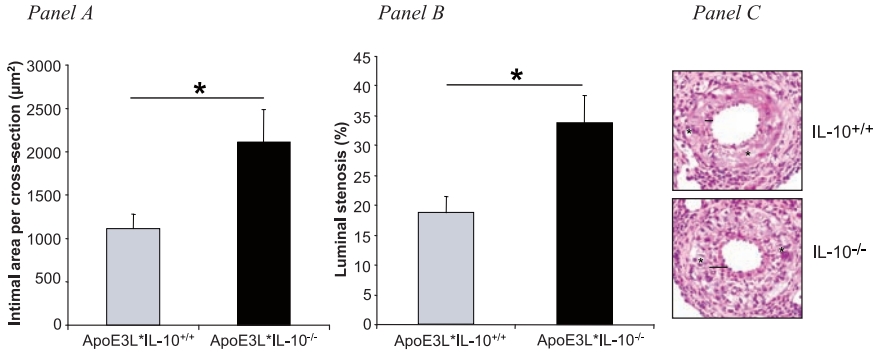

Figure 2.1. Effect of IL-10 knock-out on neointimal formation in hypercholesterolemic mice.

Total intimal thickening (Panel A) and percentage of lumenstenosis (B) of cuffed femoral arteries in APOE*3LeidenIL-10-/- and their IL-10+/+ control littermates, 14 days after cuff placement (n=8 per group, *p<0.02). Panel C represents haematoxylin-phloxine-saffron (HPS) staining of cuffed femoral arteries of both groups. Neointimal surface (indicated by black line) is clearly increased in the IL-10 knock-out group. Asterisks (*) indicate macrophage-derived foam cells (magnification 250x).

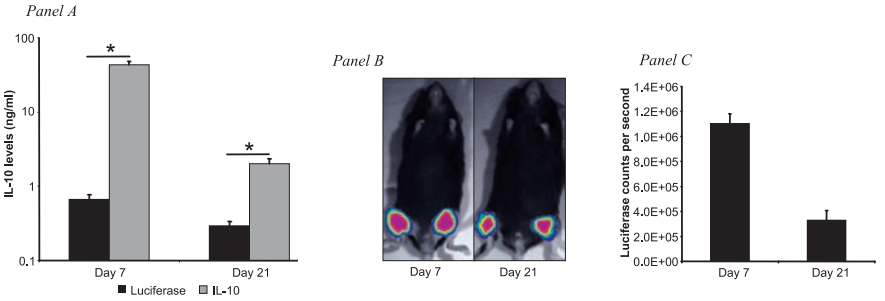

Figure 2.2. Expression of IL-10 and Luciferase after intramuscular, non-viral gene therapy.

Panel A: Murine IL 10 serum levels in ng/ml, one and three weeks after intramuscular electroporation of mIL-10 cDNA or Luciferase as a control (n=5 per group, *p<0.01). IL-10 protein levels are significantly increased as compared to the control group after electroporation at both time points. Panel B: Representative bioluminescence images of intramuscular luciferase expression at t=7 and 21 days after electrodelivery of Luciferase. Panel C: Quantitative reproduction of luciferase expression as measured with bioluminescence imaging (n=3).

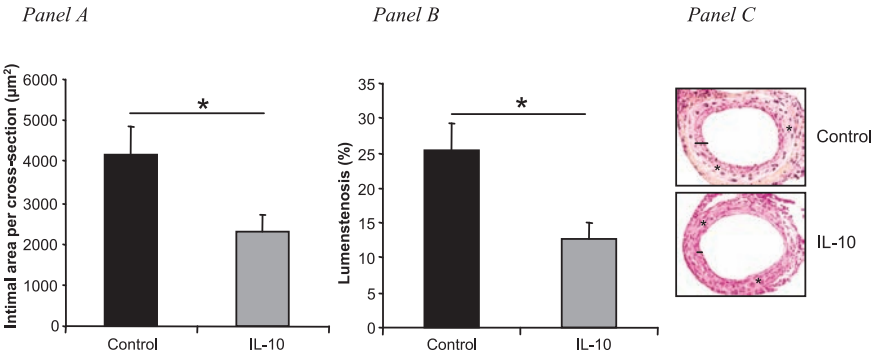

Figure 2.3. Effect of IL-10 overexpression on neointima formation in hypercholesterolemic APOE*3Leiden mice.

Total intimal area (Panel A) and percentage of lumenstenosis (B) of cuffed femoral arteries in hypercholesterolemic APOE*3Leiden mice, three weeks after electroporation of pCAGGS-mIL-10 and pCAGGS-Luciferase as a control (n=8 per group, *p<0.02). Panel C represents haematoxylin-phloxine-saffron (HPS) staining of cuffed femoral arteries after electroporation. IL-10 overexpression results in a marked reduction of neointima formation (intimal area is indicated by black line and asterisks (*) indicate macrophage-derived foam cells, magnification 200x).

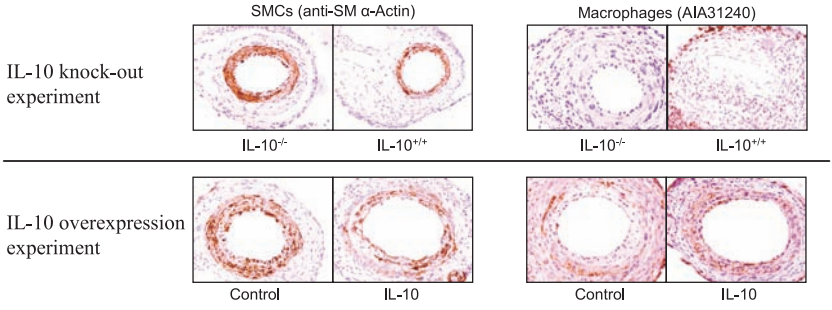

Figure 2.4. Effect of IL-10 on relative smooth muscle cell and macrophage content of medial and intimal areas.

Representative cross-sections of cuffed femoral arteries of both, IL-10 knock-out and IL-10 overexpression experiments, immunohistochemically stained for smooth muscle cells (SMCs; anti-SM α-Actin) and macrophages (AIA31240). Magnification 200x.

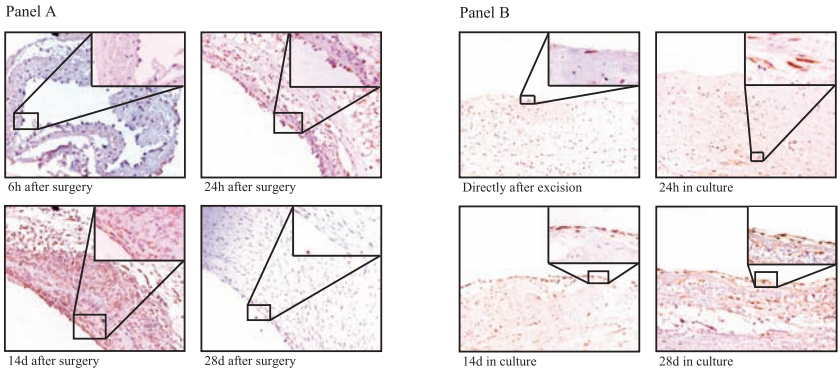

Figure 3.1. Panel A shows representative cross-sections of murine vein grafts harvested after several time points. MCP-1 expression in vein grafts identified by immunohistochemistry was seen mainly in endothelial cells, adhering monocytes and in the infiltrating cells of the developing intimal hyperplasia. Inserts indicate adhering monocytes expressing MCP-1 (6h and 24h) and MCP-1 expression in the developing intimal hyperplasia (14d).
Panel B represents the immunohistochemical detection of MCP-1 in cultured human saphenous veins. MCP-1 is abundantly present in the media at early time points and predominantly in intimal hyperplasia at later time points after 14 and 28 days. Inserts indicate MCP-1 expressing endothelium and smooth muscle cell (directly after excision and 24h) and MCP-1 expression in intimal hyperplasia (28d). Magnification of all pictures 150-600x.

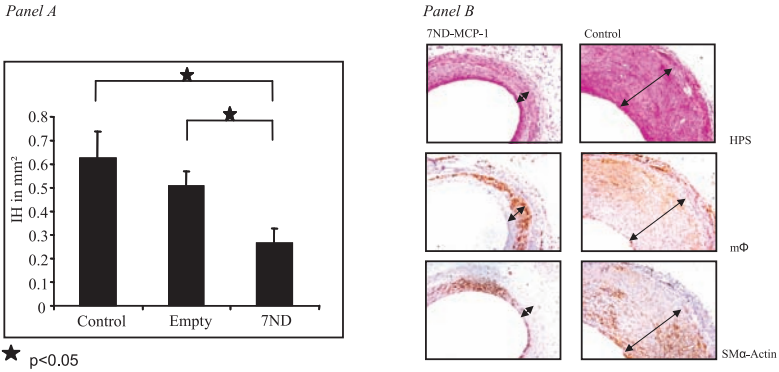

Figure 3.2. Effect of 7ND-MCP-1 gene-transfer on development of intimal hyperplasia in murine vein grafts.

Panel A: Significantly reduced intimal hyperplasia surface is seen in the 7ND-MCP-1-treated group (n=6 per group, $p<0.05$). Panel B: Immunohistochemical staining for macrophages and smooth muscle cells. No differences in cellular composition of the lesions were observed.

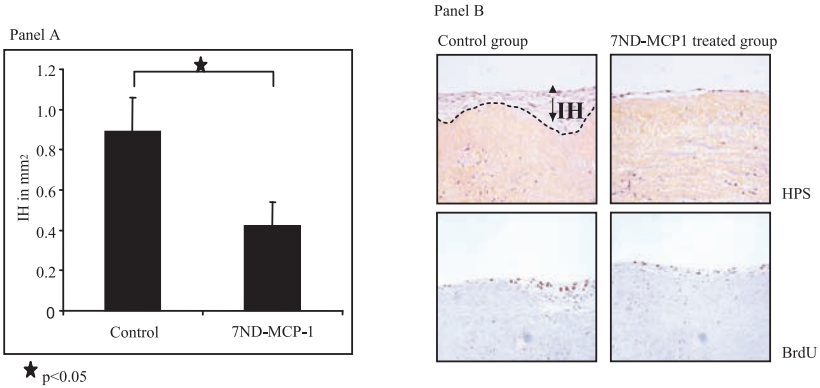

Figure 3.3. Effect of 7ND-MCP-1 on intimal hyperplasia in human saphenous vein (HSV) 28 days in culture.

Panel A: Reduction in intimal hyperplasia (n=12 per group) when exposed to conditioned medium containing 7ND-MCP-1 ($p<0.05$). Panel B: Representative cross section of human saphenous veins, strong reduction in both intimal hyperplasia surface and BrdU-positive cells can be detected.

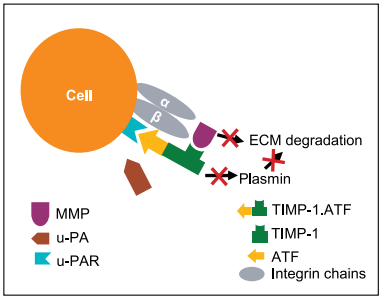

Figure 4.1. Schematic representation of the mechanism of TIMP-1.ATF.

Pericellular inhibition of plasmin and MMP activity is accomplished by anchoring TIMP-1 via ATF to the u-PA receptor. This process is enhanced by competing of TIMP-1.ATF with native u-PA for binding to u-PAR, resulting in reduction of conversion of plasminogen to plasmin and subsequently, pro-MMP activation.

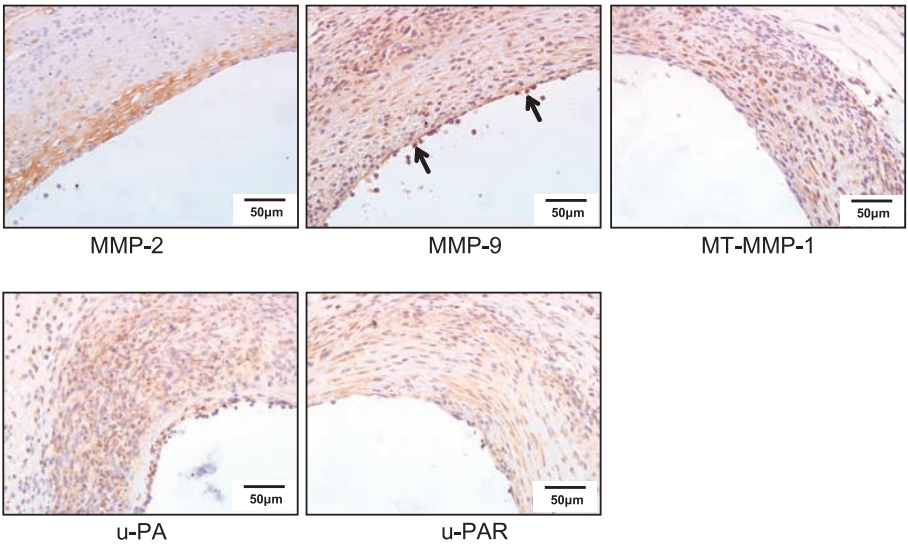

Figure 4.2. Expression of MMPs and plasminogen activator system proteases in murine vein graft.

Representative cross-sections of untreated vein grafts, harvested four weeks after surgery. MMP-2, MMP-9, MT-MMP-1, u-PA and u-PAR were visualized with specific antibodies against these proteases (see Materials and Methods for details). MMP-2 is abundantly expresses in the thickened vein graft, mainly colocalizing with smooth muscle cells. MMP-9, MT-MMP-1, u-PA and u-PAR are expressed throughout the whole vessel wall, whereas MMP-9 also can be detected in activated endothelial cells and adhering leucocytes as indicated by arrows (scale bars represent 50 µm).

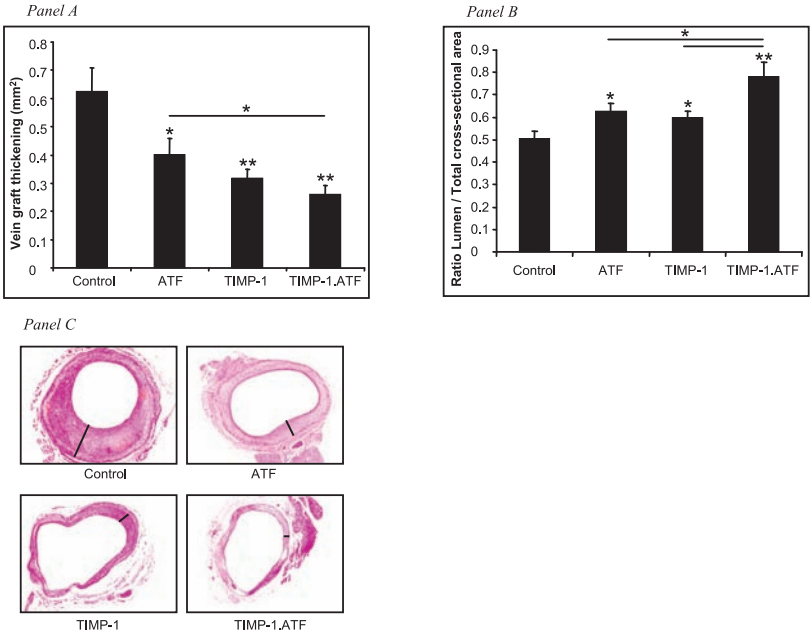

Figure 4.4. Quantification and representative HPS stained cross-sections of vein graft, 28 days after intramuscular electroporation and surgery.

Vein graft thickening and the ratio between luminal area and total vessel cross-sectional area of APOE*3Leiden mice four weeks after electroporation mediated gene transfer of pATF, pTIMP-1, pTIMP-1.mATF or pLuciferase, as a control. Vein graft surgery was performed one day after intramuscular electroporation (n=8 per group). Areas were quantified by using 6 sequential sections per segment and are expressed in millimetres squared (mean ± SEM). Treatment with all plasmids resulted in a significant reduction of vein graft thickening as compared to the control (Panel A). Ratios between the luminal area and total cross-sectional area of the vessel were significantly increased after electroporation mediated delivery of all plasmids in comparison with the control (Panel B). Also the difference between TIMP-1. mATF and the other groups was significant. Panel C represents haematoxylin–phloxine–saffron (HPS) staining of vein grafts. Although vein graft thickening is indicated by black lines, the complete circular surface was used to calculate vein graft thickened area (magnification 150x; *P<.05 **P<.01 as compared to control or indicated by black line).

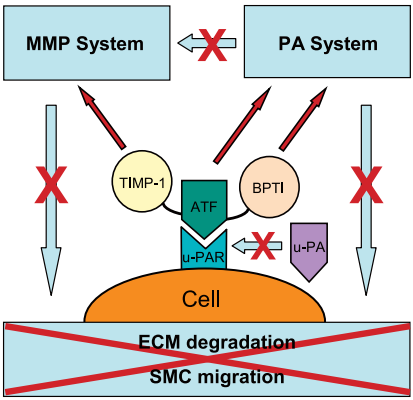

Figure 5.1. Schematic representation of the mechanism of TIMP-1.ATF.BPTI.

Anchoring TIMP-1 and BPTI by ATF to the u-PA receptor (u-PAR) locates both plasmin and MMP activity inhibiting moieties at the cell surface. TIMP-1.ATF. BPTI also competes with native u-PA for binding to u-PAR, reducing conversion of plasminogen to plasmin at the cell surface and subsequently, pro-MMP activation.

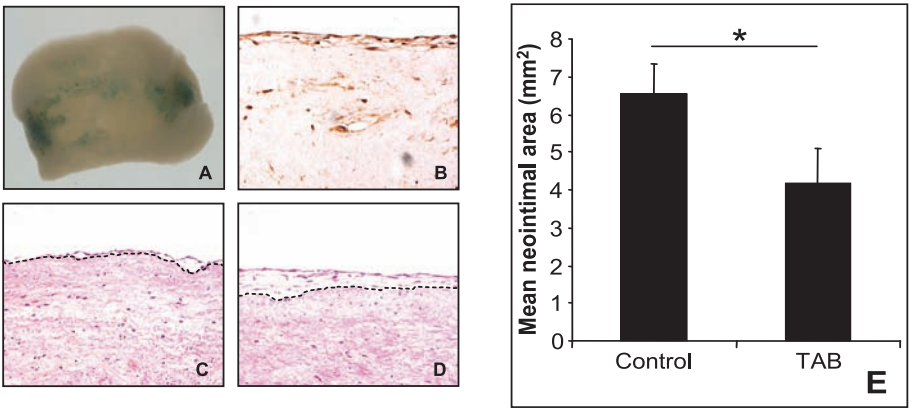

Figure 5.4. TIMP-1.hATF.BPTI inhibits vein graft thickening in explanted human vein segments.

Control vein segments were electroporated with plasmids encoding for LacZ and TIMP-1. hATF.BPTI (TAB) to assess transfection efficiency. After 28 days of culturing, vein grafts were stained with X-gal for macroscopic evaluation of ß-galactosidase activity (A) and immunohistochemistry of anti-trasylol was performed (B; counterstained with haematoxylin, magnification: 100x).
Human saphenous veins segments (n=3 per group, from 4 separate patients) were electroporated with pTIMP-1.hATF.BPTI and cultured for 4 weeks. Panel C represents an untreated control segment with a clear developed neointima. Local expression of TIMP-1.ATF.BPTI resulted in a reduction of this area (D; interrupted black line delineates neointima). Quantitative analysis of vein graft thickening was performed by image analysis on multiple sections (Panel E, expressed in mm2 per cross section (mean ± SEM); *P<.05).

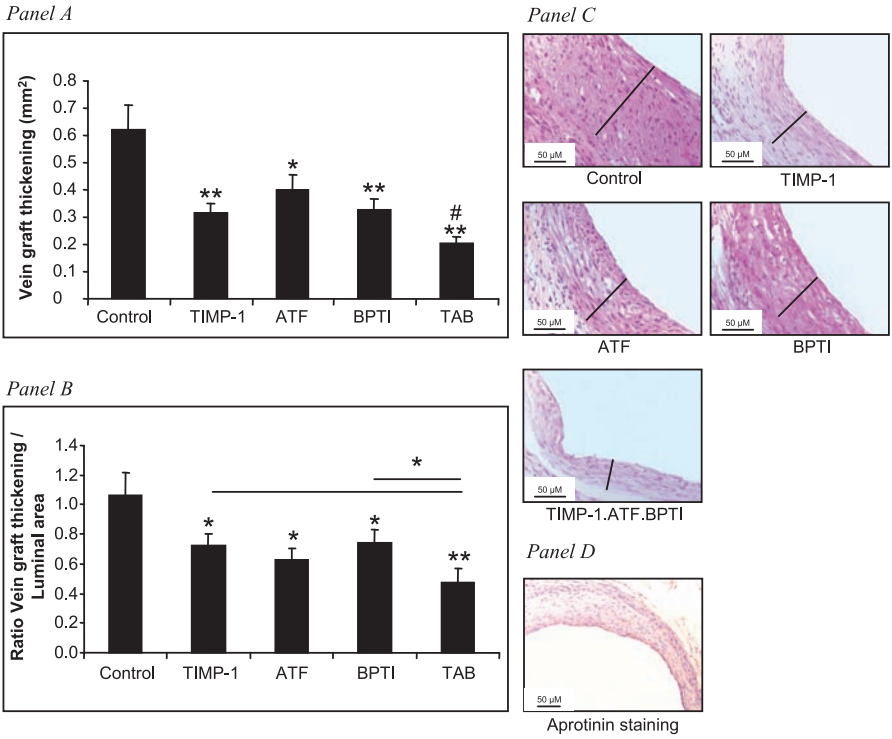

Figure 5.5. Quantitative morphometric analysis of vein graft, 28 days after intramuscular electroporation and surgery.

Hypercholesterolemic APOE*3Leiden were electroporated with TIMP-1, mATF, BPTI, TIMP-1.mATF.BPTI (TAB) or luciferase as a control and a donor vein was grafted the next day (n=8 per group). Four weeks after surgery, vein graft thickening (A) and the ratio vein graft thickening to the luminal area (B) were quantified using 6 sequential sections per segment. Areas are expressed in square millimeters (mean ± SEM). *P<.05 and **P<.008 compared with control or indicated by black line and #P<.02 compared with TIMP-1, ATF and BPTI. Haematoxylin–phloxine–saffron (HPS) staining of vein grafts is depicted in panel C (vein graft thickening is indicated by black line; magnification 250x) and TIMP-1.mATF.BPTI deposition in the vein graft is demonstrated with aprotinin immunohistochemistry (D).

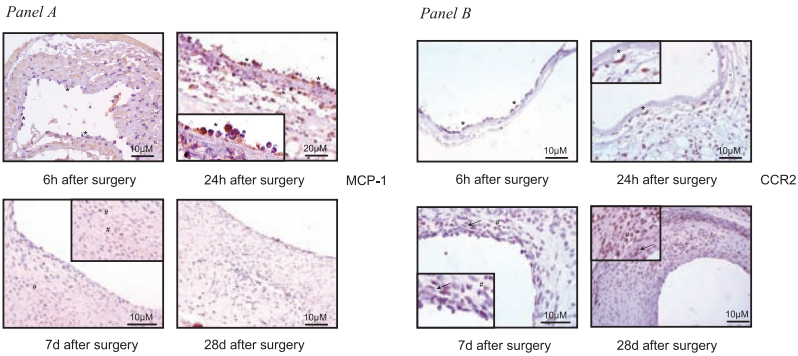

Figure 6.2. Immunohistochemical detection of MCP-1 and CCR2 in vein grafts in time.

Representative cross-sections of vein grafts harvested at 6 hours, 1, 14 and 28 days after surgery. MCP-1 (panel A) and CCR2 (panel B) expression in the vessel wall were visualized with an anti-mouse JE/MCP-1 and an anti-CCR2 antibody, respectively. MCP-1 and CCR2 expression could be detected in the adhering monocytes and in the infiltrating cells, depending of the stage of the developing vein graft thickening. Symbols indicate the several cell types (* for adhering leukocytes, # for macrophages and arrows for smooth muscle cells) and inserts represents enlargements of the specific cell types. Magnification of all images 200-400x. Scale bars represent 10 or 20 µM as indicated.

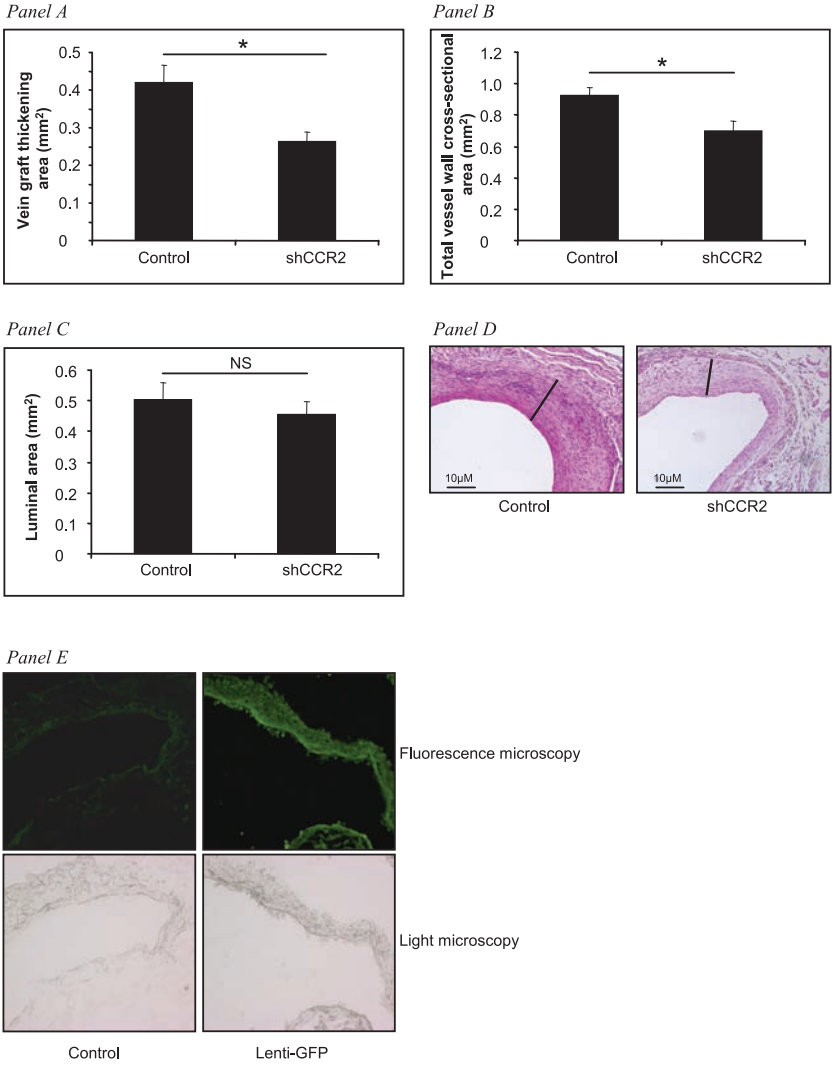

Figure 6.4. Effect of shCCR2 on vein graft thickening in hypercholesterolemic APOE*3Leiden mice.

Vein graft thickening, total vessel wall and luminal area of APOE*3Leiden mice (n=8 per group) four weeks after vein graft surgery and local infection of the vein graft with lentiviral shCCR2 or a control lentivirus. Areas were quantified by using 6 sequential sections per segment and are expressed in millimetres squared (mean ± SEM). Treatment with shCCR2 resulted in a significant reduction of vein graft thickening and total vessel wall area (Panel A and B; P=0.007). Luminal area was not affected by shCCR2 treatment (Panel C). Panel D represents haematoxylin–phloxine–saffron (HPS) staining of vein grafts (vein graft thickening is indicated by black line, magnification 200x).

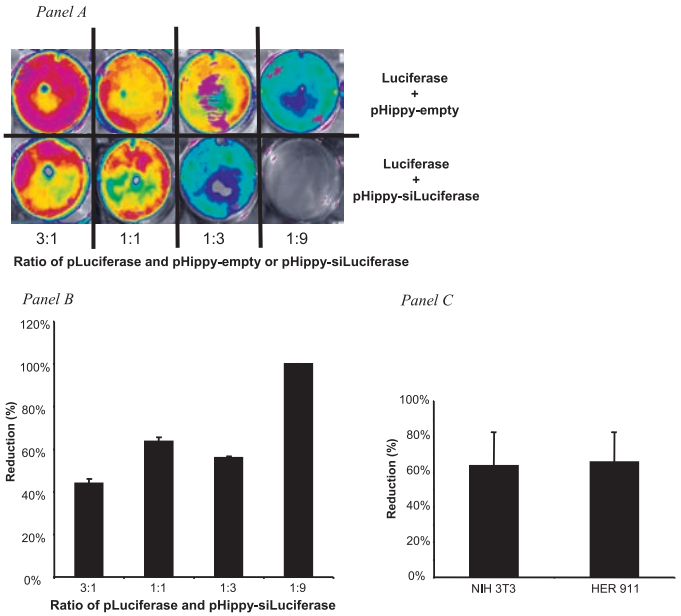

Figure 7.2. Effect of pHippy-siLuc on luciferase expression *in vitro*.

Panel A shows the luciferase expression in HER 911 cells, detected with a bioluminescence camera, one day after transfection with pcDNA3.1-Luc and pHippy-siLuc (bottom wells) or pHippy-empty as a control (upper wells) in different ratios. Panel B represents the relative reduction of luciferase expression in HER 911 cells. Sufficient luciferase expression was obtained with all ratios and the ratio 1:9 showed a complete silencing of luciferase expression. Panel C: Relative reduction of luciferase expression in NIH 3T3 and HER 911 cells after transfection with pcDNA3.1-Luc and pHippy-siLuc or pHippy-empty (ratio 1:1). In both human and murine cell types an obvious reduction of luciferase expression was monitored.

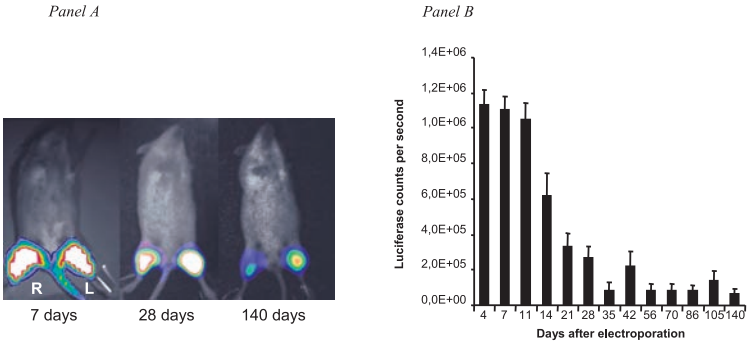

Figure 7.3. Expression of pcDNA3.1-Luc in time after electroporation of the calf muscle.

Panel A: Representative bioluminescence images of intramuscular luciferase expression at t=7, 28 and 140 days. Panel B: Quantitative reproduction of luciferase expression of all time points (n=3). Luciferase expression was detectable at least up to 140 days, but the intensity slowly declined.

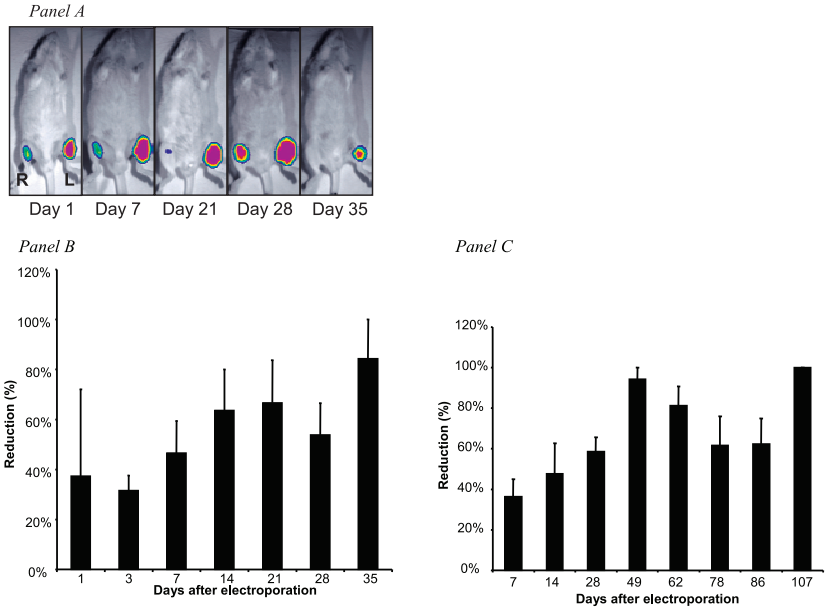

Figure 7.4. Inhibition of luciferase expression *in vivo* after treatment with pHippy-siLuc.

Panel A: Representative bioluminescence images of luciferase expression at several time points. Right legs are treated with pcDNA3.1-Luc and pHippy-siLuc, whereas left legs are electroporated with pcDNA3.1-Luc and pHippy-empty. Panel B represents the calculated silencing effect of pHippy-siLuc (n=6).
Panel C: Prolonged silencing effect of pHippy-siLuc. Reduction of luciferase expression could be measured up to 107 days after electrotransfer of pHippy-siLuc (n=3).

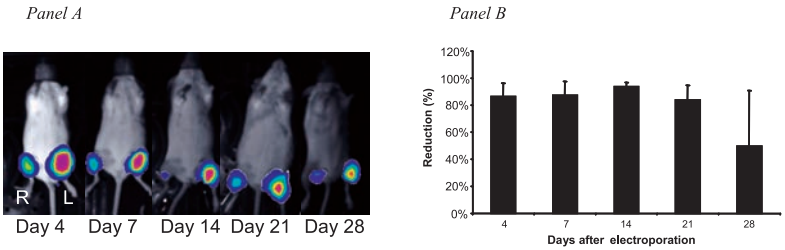

Figure 7.5. Inhibition of luciferase expression *in vivo* after electroporation with pcDNA3.1-Luc and pHippy-siLuc (right legs) and pcDNA3.1-Luc and pHippy-siScrambled (left).

Panel A: Representative bioluminescence images of luciferase expression during 1 month. Panel B represents the calculated silencing effect of pHippy-siLuc (n=3).